TECHNICAL MEMORANDUM

X-384

ANALYSIS OF TOPPING AND BLEED TURBOPUMP UNITS FOR HYDROGEN-PROPELLED NUCLEAR ROCKETS

By David G. Evans and James E. Crouse

Lewis Research Center
Cleveland, Ohio

NATIONAL AERONAUTICS AND SPACE ADMINISTRATION
WASHINGTON
June 1960

NASA TM X-384

NATIONAL AERONAUTICS AND SPACE ADMINISTRATION

TECHNICAL MEMORANDUM X-384

ANALYSIS OF TOPPING AND BLEED TURBOPUMP UNITS FOR HYDROGEN-PROPELLED NUCLEAR ROCKETS*

By David G. Evans and James E. Crouse

SUMMARY

An analysis was made of three turbopump units designed for application to a hydrogen-propelled nuclear rocket. The three units were a bleed unit, a hot-topping unit (full-flow turbine), both having turbine-inlet temperatures of 1860° R, and a cold-topping unit having a turbine-inlet temperature of 560° R. Results are presented in terms of the types of turbopump configuration required, the effects of the turbopump weight on the gross weight of the rocket, and, in the case of the bleed system, the effects of the turbine bleed on the rocket gross weight.

The results of the analysis indicated the cold-topping turbopump units were less than one-half the weight of the hot-topping units, but only slightly lighter than the bleed units. It was not within the scope of the analysis to determine which unit led to the lightest rocket. Design differences among the other components of the rocket system required by the particular turbopump unit were not evaluated.

The topping turbopump units required only single-stage turbines to drive the pumps efficiently; however, a unique blade attachment was required to prevent blade bending forces from exceeding the structural limit of the blades. The cold-topping units had a relatively small, high-speed, low-radius-ratio aluminum turbine directly coupled to a multistage axial-flow pump with a geared inducer. The hot-topping unit had a larger, low-speed, high-radius-ratio, high-temperature turbine directly coupled to an inducer stage followed by a combination centrifugal - axial-flow pump or a combination mixed-flow - axial-flow pump. The bleed units had 11-stage, axial-flow, high-speed, high-radius-ratio, high-temperature turbines coupled directly to approximately the same pump configurations as the cold-topping turbines. The optimum turbine bleed rate varied from 2.2 to 3.4 percent.

*Title, Unclassified.

INTRODUCTION

Much attention has been given to the application of nuclear energy to rocket propulsion. Generally, hydrogen has been considered as the propellant because of its low molecular weight and consequent ability to produce high values of specific impulse. In such a rocket system, gaseous hydrogen is heated in flowing through a nuclear reactor and then expanded through a rocket nozzle to produce thrust.

High system operating pressures appear likely because of the low density of hydrogen and the fact that the size and weight of the system including the reactor depend partly on its volume flow-handling capacity. In addition, for missions originating at low altitudes, elevated pressures permit larger nozzle expansion ratios and thrust.

The function of the turbopump unit is to pump hydrogen through the system at the required system operating pressure. The turbopump is not unlike those employed in present-day chemical rockets; however, the low density of hydrogen combined with the likelihood of operation at higher pressures results in more severe power requirements for the turbopump.

Several types of turbopump units are potentially suited to this application, and in this analysis three such units are investigated. They are a bleed unit and two topping units, differing in their respective turbine flow rates and turbine-inlet temperatures. The three units are shown schematically in figure 1. In the bleed unit (fig. 1(a)) liquid hydrogen is pumped from its storage area (station 0) to the nozzle and reactor shell, referred to hereinafter as the cooling jacket. The hydrogen subsequently flows through the reactor core and the nozzle (station 4 to 5) and exhausts overboard (station 6). A small fraction of the hydrogen flowing through the reactor core is bled off at a suitable turbine-inlet temperature (assumed to be 1860° R), expanded through the pump drive turbine (station 2 to 3), and then exhausted overboard through a simple converging sonic nozzle positioned to augment thrust (station 4_{tn} to 5_{tn}).

In the topping units (figs. 1(b) and (c)), liquid hydrogen is pumped through the cooling jacket and the outer annulus of a two-pass reactor core (station 1 to 2) and is thereby heated to the desired turbine-inlet temperature. Most of the flow is then expanded through the pump-drive turbine before entering the inner core of the reactor. The remainder of the flow bypasses the turbine through a turbine-bypass speed-control valve and enters the inner reactor core directly. The hot-topping unit was designed for a turbine-inlet temperature of 1860° R, the cold-topping unit for 560° R. Reactor fuel elements were assumed proportioned between the inner and outer reactor annuli to give the desired turbine-inlet temperature (station 2).

The weight of the turbopump unit is an important consideration affecting the weight and the mission capability of the rocket. Another consideration peculiar to the bleed system is the effect the bleed flow has on the available rocket specific impulse and, hence, on mission capability. In this analysis, several pump and turbine configurations are investigated for the three systems. From the investigation turbopump units are selected that exhibit the least effect on the gross weight and the mission capability of the rocket. Factors considered in determining the weight and the bleed rate of the turbopump units are turbine discharge velocity, stage number, material, rotative speed, operating pressure, and pump suction specific speed.

In the analysis, three simple vertical rocket missions are selected that result in rocket gross- to empty-weight ratios of approximately 3, 4, and 5. This range of weight ratio represents mission capabilities from that of a rocket booster to an unstaged orbital mission. In addition, a range of rocket base structural parameter of 0.10 to 0.20 and rocket chamber pressures of 700 to 1300 pounds per square inch are considered. Rocket chamber temperatures are held constant at 3960° R.

The analysis does not include the effects each turbopump unit has on the weights of other components of the system, such as the reactor. The analysis considers only the configurations and weights of the turbopump units, their subsequent effect on rocket specific impulse, where present, and rocket gross weight.

SYMBOLS

A	area, sq ft
c_p	specific heat at constant pressure, Btu/(lb)(°R)
D	turbine blade tip diameter, ft
G	ratio of rocket thrust at sea level to initial gross weight
g	acceleration due to gravity, 32.2 ft/sec^2
H	altitude, ft
H_{sv}	suction head, ft
Δh	specific work, Btu/lb
I	nozzle specific impulse, lb-sec/lb
I^*	available rocket specific impulse, lb-sec/lb

J	mechanical equivalent of heat, 778.16 ft-lb/Btu
K	turbine weight factor (eq. (8))
N	rotative speed, rpm
n	number of turbine stages
P	rocket payload, lb
p	absolute pressure, lb/sq ft (except where noted)
Q	flow rate, gal/min
R	gas constant, ft/$^{\circ}$R
r_h/r_t	turbine blade hub- to tip-radius ratio
S	structural parameter, structural weight/propellant weight
$\overline{S}$	base structural parameter, $S - \frac{W_{tp}}{W_P}$
ss	suction specific speed
T	temperature, $^{\circ}$R
t	time, sec
U	blade tip speed, ft/sec
V	velocity, ft/sec
W	weight, lb
w	weight-flow rate, lb/sec
y	ratio of turbine to pump weight-flow rate
γ	ratio of specific heats
δ	rocket-control and nozzle-velocity correction factor
ϵ	turbine exhaust thrust recovery coefficient, I_{tn}/I_{rn}
η_p	overall pump efficiency
η_t	turbine efficiency based on turbine total- to static-pressure ratio

$\overline{\eta_t}$ turbine efficiency based on turbine total- to total-pressure ratio

ρ density, lb/cu ft

Subscripts:

B bleed unit

BO burnout

CT cold-topping unit

cr critical

e empty

F frontal

f final

G inducer gearing

g gross

HT hot-topping unit

P propellant

p pump

rn rocket nozzle

sl sea level

T topping units

t turbine

tn turbine exhaust nozzle

tp turbopump

u tangential component

x axial component

0 pump inlet

1 pump discharge

2 turbine inlet

3 turbine exit

3a inlet to reactor inner core

4 nozzle chamber

5 nozzle exit

6 atmospheric

Superscript:

' total conditions

METHOD OF ANALYSIS

System Operating Conditions

The three types of turbopump unit investigated along with their associated system components are considerably simplified where possible to facilitate the analysis (fig. 1). The assumed operating temperatures, pressures, and flow rates are noted in table I. Selection of the values was arbitrary; however, they were either representative of or within the feasible limits of the systems. The thermodynamic properties of hydrogen were either assumed or obtained from reference 1. The sum of all pressure drops incurred in circulating the hydrogen through the lines, cooling jacket, and reactor core were estimated to be approximately equal for each system. The actual magnitudes selected and held constant throughout the analysis are given in table II. The pressure drop across the bypass valve in the topping units is assumed to equal the drop in pressure across the turbine. The resulting pump pressure rise required for the units is given in table III. For the topping units, the overall turbine pressure ratio p_2'/p_{3a}' affects the required pump pressure rise necessary to satisfy p_4'.

Rocket-Turbopump Relations

The ratio of the gross weight of a rocket to its payload W_g/P is a function of the gross- to empty-weight ratio W_g/W_e and the structural

parameter S according to the equation (eq. (10), ref. 2)

$$\frac{W_g}{P} = \frac{W_g/W_e}{1 - S\left(\frac{W_g}{W_e} - 1\right)} \tag{1}$$

where S is defined as the ratio of the structural weight of the rocket to the propellant weight, that is,

$$S = \frac{W_e - P}{W_P} \tag{2}$$

The weight of the turbopump component of the rocket W_{tp} is an incremental part of the empty weight W_e, and thus

$$S = \frac{W_{reactor} + W_{tank} + \cdots + W_{tp}}{W_P} \tag{3}$$

or

$$S = S_{reactor} + S_{tank} + \cdots + \frac{W_{tp}}{w_p t_{BO}} \tag{4}$$

where it is assumed that all the propellant is used in flight

$$W_P = w_p t_{BO} \tag{5}$$

Combining all the components of the rocket except the turbopump into one term, $\bar{S}$, defined as the base structural parameter, and rewriting equation (4) separate the effect of the turbopump weight on the rocket structural parameter from that of the other components:

$$S = \bar{S} + \frac{W_{tp}}{w_p t_{BO}} \tag{6}$$

In the solution of equation (6), a range of values of $\bar{S}$ from 0.10 to 0.20 is assumed, which is considered representative of future hydrogen-propelled nuclear rockets. Turbopump weights W_{tp} are obtained as a ratio of the pump weight flow W_{tp}/w_p in the next section, Turbopump Considerations. Finally, the burnout time t_{BO}, which is a function primarily of the rocket mission and specific impulse, is developed in the section Rocket Mission Considerations.

The bleed turbopump unit also affects W_g/P (eq. (1)) through the effect the turbine drive fluid has on the available specific impulse I^* and, therefore, the W_g/W_e of the rocket. This effect is considered in developing the equations for t_{BO} and W_g/W_e in the section Rocket Mission Considerations.

Turbopump Considerations

The weight of the turbopump unit includes the combined weights of the turbine, pump, and inducer gearing, when gearing is necessary. The weight of each part is obtained separately as a ratio of the pump weight flow w_p and then combined in the ratio W_{tp}/w_p required for equation (6):

$$\frac{W_{tp}}{w_p} = \frac{W_t}{w_p} + \frac{W_p}{w_p} + \frac{W_G}{w_p} \tag{7}$$

Bleed turbine. - The procedure used to obtain $(W_t/w_p)_B$ (eq. (7)) for the bleed turbine is taken from reference 2. In this reference, turbine weight characteristics are analyzed in terms of the required turbine specific work $\Delta h'$, bleed rate y, blade speed U, number of stages n, radius ratio r_h/r_t, pressure ratio p_3/p_2', efficiency η, and stress.

In equation (14) of reference 2, the weight of the turbine is expressed as a function of the turbine frontal area, number of stages, and turbine material as accounted for in the term K. The equation was developed as the result of several comprehensive turbine weight studies and is rewritten here as

$$W_{Bt} = Kn^{1/2}A_F \tag{8}$$

or, dividing through by w_p,

$$\left(\frac{W_t}{w_p}\right)_B = Kn^{1/2}\frac{A_F}{w_p} \tag{9}$$

Equations (16) to (33) of reference 2 were then combined to obtain $(A_F/w_p)_B$ in terms of the turbine operating variables and substituted into equation (9) to give

$$\left(\frac{W_t}{w_p}\right)_B = \frac{Ky\sqrt{nT_2'}\sqrt{1 - \frac{\Delta h'}{c_p T_2'}}\left\{1 - \frac{\gamma - 1}{\gamma + 1}\left[\left(\frac{V_x}{V_{cr}}\right)_3^2 + \left(\frac{V_u}{V_{cr}}\right)_3^2\right]\right\}}{p_2'\sqrt{\frac{2\gamma g}{(\gamma + 1)R}}\left(\frac{V_x}{V_{cr}}\right)_3\left[1 - \left(\frac{r_h}{r_t}\right)_3^2\right]\left(\frac{p_3}{p_2'}\right)} \tag{10}$$

The exit whirl leaving the last stage of the turbine $(V_u/V_{cr})_3$ is obtained from equations (34) to (37) of reference 2. The required specific-work output, needed for equation (10), is a function of the pump requirements

$$\Delta h' = \frac{\Delta p_p'}{y\rho_p\eta_p J} \tag{11}$$

The required turbine pressure ratio p_3/p_2' is obtained from

$$\frac{p_3}{p_2'} = \left(1 - \frac{\Delta h'}{c_p T_2' \eta_t}\right)^{\gamma/\gamma - 1} \tag{12}$$

where η_t is the turbine static efficiency based on the ratio of inlet total to exit static pressure. Values of static efficiency are obtained from efficiency curves presented in references 2 and 3 relating efficiency to turbine work, speed, and number of stages. These curves are based on a study of turbine velocity diagrams and loss considerations. In the study, equal work and blade speed were assumed for each stage, reheat effects were neglected, and constant loss coefficient and stator-exit flow angle were assumed that were within the range of values suitable for this turbopump application. One factor not considered in the efficiency curves of references 2 and 3 was the effect of Reynolds number on efficiency. Since there are no extremes represented in the size of turbines being considered, the effect of size on Reynolds number is considered small enough to neglect. Similarly, the effects on Reynolds number caused by the range of pressures covered in the analysis are considered small enough to neglect.

The conditions given in table IV are assumed in the solution of $(W_t/w_p)_B$ for the bleed turbine. The blade speed and exit radius ratio selected corresponded to a disk taper of 4 and a maximum untapered blade and disk centrifugal stress of 38,000 pounds per square inch. Rotor material is assumed to be high-temperature alloy steel.

The turbine weight parameters required for the bleed turbopump units were computed from equations (10) to (12) for the conditions and variables

shown in table IV. Preliminary plots of $(W_t/w_p)_B$ against y were made for each value of n and p_4' considered, from which minimum-turbine-weight envelope curves were constructed. These curves are shown plotted in figure 2 against bleed rate for the three chamber pressures considered. The number of turbine stages required at each point on the curves is also indicated in the figure.

Topping turbines. - The equations and the procedure used to obtain $(W_t/w_p)_T$ (eq. (7)) for the topping turbines is the same as that for the bleed turbine with the exception of equation (12) for turbine pressure ratio. The topping pressure ratios are obtained from the following equation:

$$\left(\frac{p_3}{p_2'}\right)_T = \frac{p_3}{p_3'}\frac{p_3'}{p_2'} \tag{13}$$

where

$$\frac{p_3}{p_3'} = \left[1 - \frac{\gamma - 1}{\gamma + 1}\left(\frac{V_x}{V_{cr}}\right)_3^2\right]^{\gamma/\gamma-1} \tag{14}$$

assuming zero exit whirl, and where

$$\frac{p_3'}{p_2'} = \left(1 - \frac{\Delta h'}{c_p T_2' \bar{\eta}_t}\right)^{\gamma/\gamma-1} \tag{15}$$

The turbine total efficiency $\bar{\eta}_t$ is based on the ratio of inlet to exit total pressure and is obtained from equation (16) of reference 3. This equation was derived from considerations of the same turbine operating variables as used to derive static efficiency, noted in the previous section. Total efficiency is used because the specific-work output of the topping turbines is small compared with the kinetic energy leaving the turbine. By comparison, the specific-work output of the bleed turbines is high, and therefore static efficiency could be used. The total pressure of the flow leaving the topping turbines and entering the inner reactor core p_{3a}' is considered as either completely recovered where $p_{3a}' = p_3'$ (case 1) or completely lost where $p_{3a}' = p_3$ (case 2);

$$\frac{p_2'}{p_{3a}'} = \frac{p_2'}{p_3'} \qquad \text{(Case 1)} \tag{16}$$

$$\frac{p_2'}{p_{3a}'} = \frac{p_2'}{p_3} \qquad \text{(Case 2)} \tag{17}$$

The pressure ratios p_2'/p_{3a}' affect the pump pressure rise $\Delta p_p'$ (table III) required to satisfy the given chamber operating pressures. Therefore, an iterative process is required to match the turbine pressure ratio p_3'/p_2' and specific-work output $\Delta h'$ (eq. (15)) with the actual work required to drive the pump (eq. (11)).

The conditions given in table V are assumed in the solution of $(W_t/w_p)_T$ for the topping turbines. The blade-speed and exit-radius ratios selected correspond to an untapered blade centrifugal stress of 23,000 and 38,000 pounds per square inch, respectively, for the cold and hot turbines. Higher blade-speed and exit-radius ratios than those noted were not considered, because it was observed that to maintain the same operating stress turbine weight increased while rotative speed remained constant.

The turbine weight parameters $(W_t/w_p)_{HT}$ required for the hot-topping turbopump units were therefore obtained by the iterative solution of equations (10) and (11) and (13) to (17). The results are shown in figure 3(a) plotted over the given ranges of turbine-exit velocity ratio $(V_x/V_{cr})_3$ and chamber pressure p_4' for the exit conditions of cases 1 and 2. The turbines were single-stage units and had a flow rate of 80 percent of that of the pump, a blade tip speed of 1400 feet per second, and an inlet temperature of 1860° R. The result of increasing the chamber pressure from 700 to 1300 pounds per square inch absolute was to reduce the turbine volume flow rate and size and therefore the turbine weight. In like manner, losing the velocity head leaving the turbine (case 2) increased the turbine operating pressure over that of case 1 and thus permitted a smaller and lighter turbine. Finally, increasing $(V_x/V_{cr})_3$ increased the unit flow-handling capacity of the turbine to further reduce its size and weight.

Single-stage turbines were aerodynamically capable of delivering the required pump work; therefore, turbine weights were not affected by variations in turbine work over the range of chamber pressure and turbine variables considered. However, the amount of work required from the single-stage turbines imposed a severe bending component of stress on the rotor blading, giving a combined stress beyond the material limits of the blading. Therefore, the assumption was made that blade attachments could allow for enough blade lean to counterbalance the bending component with a centrifugal component. Lean angles up to 2° from radial appeared sufficient to accomplish this, depending on the particular rotor design.

The cold-topping turbine weight parameters were obtained the same way as the hot-topping parameters. Figure 3(b) presents the turbine

weight parameters over the range of system variables considered. Only single-stage turbines were required; however, no turbine solutions were possible for the chamber pressure of 1300 pounds per square inch absolute. The required pumping powers exceeded the available energy of the turbine driving fluid. Increasing turbine efficiency by multistaging the turbine brought the actual turbine work closer to the required turbine output; however, an increase in the assumed turbine-inlet temperature would have been required before a solution was possible.

Turbine weights average one-tenth those of the hot-topping turbines because of the use of aluminum rather than steel and smaller frontal areas made possible by a lower permissible blade radius ratio and lower volume flow rate. The combined blade stress using the single-stage turbine exceeded the material limits of the aluminum; therefore, the same assumption was made as for the hot-topping turbines, that blade lean could be incorporated to counterbalance blade bending.

Pumps. - The pump weight parameters W_p/w_p required for equation (7) were obtained from a study of pump design and pump weight characteristics, the results of which are presented in figure 4. Pump designs were made for three values of Δp_p^i, arbitrarily selected as 900, 1300, and 1700 pounds per square inch, over a range of shaft speeds from 6000 to 21,000 rpm. Only multistage pump designs were considered, and they involved the use of various combinations of inducer, axial, mixed, and centrifugal stages. The following discussion covers the considerations and limitations that were made to determine the pump configurations and resulting weight parameters.

Direct-drive pumps were used to eliminate the weight of gearing between the turbine and the pump, which at the high power levels required for pumping hydrogen can be as heavy as or heavier than the pumps themselves. The pumps were therefore driven at the turbine rotative speed, which defined in terms of turbine parameters (eq. (9)) is

$$N_p = N_t = \frac{60U_t}{\pi D_t} = \frac{60U_t}{\sqrt{4\pi A_{F,3}}} = \frac{60U_t}{\sqrt{\frac{4\pi}{K\sqrt{n}} \frac{W_t}{w_p} w_p}} \tag{18}$$

However, the high rotative speeds of direct-drive pumps can make their suction specific speeds excessively high:

$$ss = \frac{N_p\sqrt{Q}}{(H_{sv})^{3/4}} \tag{19}$$

where H_{sv} is limited by tank pressure p_0. The design H_{sv} was set at 652 feet, corresponding to 20 pounds per square inch.

Suction specific speed is the parameter that indicates the point of inception of cavitation, and to some extent the severity of cavitation. Cavitation begins at suction specific speeds around 10,000 for well designed pumps and becomes more fully developed at values above this. Cavitation, especially in the more fully developed form, impairs pump performance. In such instances, an inducer stage can be used to increase H_{sv} enough under cavitating conditions that the following loaded stages of the pump operate cavitation free. Because suction specific speeds exceeded 10,000 over the range of pump speed and flow rate considered in the analysis, an inducer stage was used. At suction specific speeds above 30,000 it was not certain what pressure rise could be developed in the inducer. Therefore, in these instances the inducer was geared down to prevent suction specific speeds from exceeding 30,000. The weight of the inducer stage was included as part of the pump weight parameter. The inducer gearing weight parameter W_G/w_p was considered separately (eq. (7)). Weights were estimated at 0.02 pound per horsepower transmitted, which was considered a conservative estimate as compared with several unpublished gearbox weight analyses made in the range of power encountered with the subject inducers.

The high operating pressures and, hence, $\Delta p_p'$ required for the rocket systems considered, and the desirability of having a small number of pump stages requires a high pressure rise per stage. The pressure rise per stage for the case of no inlet whirl is proportional to the product $(U_1)\Delta V_u$. Radial bladed centrifugal pump stages were used to develop most of the pressure rise in the 6000 to 10,000 rpm speed range, where ΔV_u was assumed equal to $0.9\ U_1$. A maximum value of U_1 of 1200 feet per second was used, based on blade stress considerations. In addition, a minimum outlet- to inlet-diameter ratio of 2 was used, based on blade hydrodynamic loading considerations. The loaded-pump-stage inlet diameter was made approximately equal to the inducer diameter because of cavitation considerations. Calculations indicated that the optimum inducer diameter and, hence, pump-inlet diameter remained nearly constant over a wide range of speeds for given values of Q, H_{sv}, and hub- to tip-diameter ratio. Hence, the outlet- to inlet-tip-diameter ratio was reduced as the rotative speed was increased for the given tip speed. A rotative speed of 10,000 rpm was the speed at which the pump outlet- to inlet-tip-diameter ratio reached the assumed limiting value of 2.

Loaded mixed-flow stages were used to develop most of the required pressure rise in the range of rotative speed from 10,000 to 14,000 rpm. A mixed-flow stage can develop the same pressure rise as several axial-flow stages and is probably slightly lighter than an axial-flow pump

developing the same pressure rise. The mixed-flow pump outlet- to inlet-tip-diameter ratio was arbitrarily selected as 1.4. The pumps had the same inlet conditions as the centrifugal pumps. Centrifugal stress limited the speeds of the mixed-flow pumps to a maximum speed of 14,000 rpm, for which the outlet- to inlet-tip-diameter ratio of 1.4 could be maintained. At rotative speeds above 14,000 rpm, axial-flow pumps were used.

The pump weight parameters were calculated from the centrifugal, mixed-flow, and axial-flow pump weight parameters presented in reference 4. The design conditions and the resulting pump and thrust balancing weights for the pumps of reference 4 are tabulated in table VI. The weight of balance pistons is included in the term W_p/w_p. The pump weight parameters were then corrected to a flow rate of 800 pounds per second (table I) by multiplying the reference pump weight parameters (table VI) by the ratio of the respective pump weight flows to the 1.2 power $((w_p/w_{p,ref.})^{1.2})$. This correction appears optimistic according to the square-cube law, but, realistically, it matched more closely the trends of pump weight with weight flow exhibited by existing pumps. The pump weight parameters were assumed to vary linearly with pressure rise and inversely with rotative speed squared for a fixed tip speed. When two pump types were staged together, the stage weight parameters of the corresponding reference stages were scaled for speed and weight flow and then added together to obtain the overall pump weight parameter.

Plots of the resulting pump weight parameters against speed are shown in figure 4 for the three values of $\Delta p_p'$ considered, 900, 1300, and 1700 pounds per square inch. Some uncertainty existed as to the exact magnitude of the resulting curves because of the arbitrary methods used to determine them. However, the trends of the pump weight parameter with respect to speed, pressure rise, and configuration are representative.

The parameter for pump plus inducer gear weight $(W_p + W_G)/w_p$ (eq. (7)) was then obtained directly from figure 4 for each speed (eq. (18)) and pressure rise (table III) resulting from each turbine configuration and variable specified in the previous turbine sections. Values of $\Delta p_p'$ were interpolated between the given curves in figure 4, which gave sufficiently accurate results for purposes of the analysis. The number and the type of pump stages were also interpolated between curves by assuming a linear variation in the number of axial stages between the curves.

Rocket Mission Considerations

Three missions are considered that are simple vertical missions originating at the earth's surface. No aerodynamic drag or variation in gravity with altitude is assumed. The missions consist of a vertical acceleration during rocket firing, and then a vertical deceleration due to gravity to a maximum altitude H_f, where rocket velocity V_f is zero. Specification of the three missions requires selection of a thrust to gross-weight ratio at takeoff G and three values of H_f. As noted in the INTRODUCTION, the selection of H_f is so made that the resulting values of rocket W_g/W_e are approximately 3, 4, and 5. The value for G is arbitrarily specified as 1.4; that is,

$$G = \frac{(I^*_{sl})w_p}{W_g} = 1.4 \tag{20}$$

which results in a takeoff acceleration of 12.9 feet per second per second.

The following equations are used to relate the mission and rocket characteristics. The relation between burnout and final altitude H and velocity V is

$$H_f - H_{BO} = \frac{V_{BO}^2 - V_f^2}{2g} \tag{21}$$

which, for V_f equal to zero is

$$H_f = H_{BO} + \frac{V_{BO}^2}{2g} \tag{22}$$

The altitude and the velocity are also functions of time t, as derived in the following vertical-flight equation relating the forces acting on the rocket to its acceleration and weight:

$$I^*w_p - (W_g - w_p t) = \left(\frac{W_g - w_p t}{g}\right)\frac{dV}{dt} \tag{23}$$

Combining equations (20) and (23) and rewriting in delta form gives

$$\Delta V = g\left(\frac{I^*}{\frac{I^*_{sl}}{G} - t} - 1\right)\Delta t \tag{24}$$

[redacted]

where

$$t = \sum \Delta t \tag{25}$$

The altitude and velocity can then be found at any time t during the mission using equation (24) and the following relations

$$V = \sum \Delta V \tag{26}$$

$$H = \sum \Delta H$$

$$= \sum \left[\left(V + \frac{\Delta V}{2}\right)\Delta t\right] \tag{27}$$

The solution of equation (24) involves a step integration of velocity with respect to time. Step intervals of 1-second duration are taken up to values of t where V and H (eqs. (26) and (27)) satisfy H_f (eq. (22)). At this point, t is specified as t_{BO}.

Also required in the solution of equation (24) is knowledge of the available rocket specific impulse I^* during the mission. Because the specific impulse is a function of the mission altitude and, therefore, time, an iterative process is required at each step of the integration to maintain the correct relation between I^*, H, and t.

The equation for nozzle specific impulse I, as used from reference 5, is

$$I = \left[\frac{V_5}{g} + \frac{A_5}{w_5}(p_5 - p_6)\right]\delta \tag{28}$$

where, for the converging-diverging rocket nozzle, assuming isentropic flow and negligible chamber velocity,

$$V_{5,rn} = \sqrt{\frac{2\gamma g R T_4'}{\gamma - 1}\left[1 - \left(\frac{p_5}{p_4}\right)^{\gamma-1/\gamma}\right]} \tag{29}$$

and

$$\left(\frac{A}{w}\right)_{5,rn} = \left(\frac{1}{\rho V}\right)_5 = \frac{1}{\left(\frac{\rho V}{\rho' V_{cr}}\right)_5 (\rho' V_{cr})_5} \tag{30}$$

which expands to

$$\left(\frac{A}{w}\right)_{5,rn} = \frac{\frac{\gamma + 1}{2\gamma}\left(\frac{A}{A_{cr}}\right)_5 \sqrt{\frac{2\gamma}{\gamma + 1} gRT'_4}}{p'_5 g\left(\frac{2}{\gamma + 1}\right)^{1/\gamma - 1}} \tag{31}$$

The value of γ is assumed constant at its chamber value (station 4). A correction factor δ for equation (28) of 0.94 is assumed to account for rocket directional control losses and nozzle velocity losses. Full nozzle expansion ($p_5 = p_6$) is assumed to occur at an altitude of 50,000 feet, and nozzle critical area ratios $(A/A_{cr})_5$ (eq. (31)) are computed for this altitude. Nozzle losses due to nozzle overexpansion below this altitude are approximated by assuming p_5 remains constant at its 50,000-foot value (ref. 5). The variation of atmospheric pressure p_6 (eq. (28)) with altitude is also obtained from reference 5.

For the converging sonic nozzle used with the bleed turbopump unit, the terms in equation (28) become

$$V_{5,tn} = \sqrt{\frac{2\gamma}{\gamma + 1} gRT'_{4,tn}} \tag{32}$$

$$\left(\frac{A}{w}\right)_{5,tn} = \frac{\frac{\gamma + 1}{2\gamma} V_{5,tn}}{gp'_{5,tn}\left(\frac{2}{\gamma + 1}\right)^{1/\gamma - 1}} \tag{33}$$

and

$$p_{5,tn} = \frac{p_{4,tn}}{\left(\frac{\gamma + 1}{2}\right)^{\gamma/\gamma - 1}} \tag{34}$$

For this nozzle, a value of δ of 0.97 is used to correct for nozzle velocity error. Nozzle temperatures $T'_{4,tn}$ are obtained from the turbine-inlet temperature T'_2, the specific-work output $\Delta h'$, equation (11), and the assumptions that $T'_{4,tn}$ equals T'_3 and that c_p remains constant between stations 2 and 3:

$$T'_{4,tn} = T'_3 = T'_2 - \frac{\Delta h'}{c_p} \tag{35}$$

The total available rocket specific impulse I^* required in the solution of equation (24), therefore, becomes a function of the turbopump unit considered. For the bleed unit (ref. 2)

$$I^* = I_{rn}[1 - (1 - \epsilon)y] \tag{36}$$

where y represents the percent of total flow bled from the reactor to drive the turbine. The term ϵ represents the ratio of specific impulse achieved in the turbine exhaust nozzle to that obtained in the main rocket nozzle,

$$\epsilon = \frac{I_{tn}}{I_{rn}} \tag{37}$$

For the system incorporating the topping turbopump units, the available specific impulse is simply

$$I^* = I_{rn} \tag{38}$$

It is noted previously that three values of H_f (eq. (22)) were required such that the rocket gross- to empty-weight ratio W_g/W_e approximates values of 3, 4, and 5. Once the mission altitude and velocity are known as a function of time and the available specific impulse is known as a function of altitude, values of W_g/W_e can be obtained from equation (9) of reference 2, rewritten here as

$$\frac{W_g}{W_e} = \left[1 - G\left(\frac{t_{BO}}{I^*_{sl}}\right)\right]^{-1} \tag{39}$$

It has been shown that selection of the three missions required only the selection of a thrust to gross-weight ratio at takeoff $G_{}$ of 1.4 and three values of H_f. The three values selected were 65×10^5, 110×10^5, and 155×10^5 feet which, as will be shown, resulted in rocket gross- to empty-weight ratios W_g/W_e of approximately 3, 4, and 5.

Full nozzle expansion was assumed to occur at a 50,000-foot altitude, and to satisfy this condition, nozzle area ratios $(A/A_{cr})_5$ of 26.7, 35.2, and 43.0 were required for the three chamber pressures of 700, 1000, and 1300 pounds per square inch absolute, respectively. The resulting values of specific impulse achieved in the rocket nozzle I_{rn} (eq. (28)) are shown plotted against altitude H and chamber pressure p'_4 in figure 5. The figure illustrates the effects that H and p'_4 had on the available expansion and, therefore, on the specific impulse of the hydrogen. The specific impulse achieved at the 50,000-foot altitude

ranged from 735 to 753 lb-sec/lb for chamber pressures of 700 to 1300 pounds per square inch, respectively. Rocket thrusts at this altitude for a hydrogen flow rate of 800 pounds per second were, therefore, 588,000 and 602,000 pounds, respectively.

The total available specific impulse I^* for the rocket mission using the topping turbopump units was equal to the specific impulse of the single converging-diverging nozzle I_{rn} (fig. 4). These values were therefore used in the step solution of equations (22) to (27) for the three topping missions and chamber pressures. The mission burnout times t_{BO} and rocket gross- to empty-weight ratios W_g/W_e (eq. (39)) resulting from the calculations are given in table VII. The bleed flow required during the rocket missions using the bleed turbopump unit reduced the available specific impulse of the rocket from the values obtained for the topping systems (fig. 5). The exact reduction depended on the amount of bleed and the amount of specific impulse recovered from the turbine exhaust ϵ (eqs. (36) and (37)). An iterative solution was required between mission equations (24) to (37) to maintain the correct relation between the available specific impulse and altitude at each second during the mission. The resulting mission burnout times t_{BO} satisfied the three values of H_f of 65×10^5, 110×10^5, and 155×10^5 feet (eq. (22)) and are shown plotted (fig. 6(a)) over the given range of chamber pressure and bleed rate. The burnout times and sea-level values of available specific impulse were then used with equation (39) to obtain W_g/W_e (fig. 6(b)). It may be noted in the figure that the range of three missions selected resulted in values of W_g/W_e nearly equal to 3, 4, and 5, respectively.

E-381

CC-3 back

Calculation Procedure

The procedure for using the equations presented herein may be further illustrated by two example calculations, one for a bleed turbopump design and the other for a cold-topping turbopump design. In both examples, a representative value is selected for each of the turbine and mission variables considered in the analysis.

Bleed turbopump design. - The values considered for the example bleed system are given in table VIII along with the procedure and results of the example.

Cold-topping turbopump design. - The values considered for the example cold-topping system, the procedure, and the results of the example are given in table IX.

[redacted]

RESULTS AND DISCUSSION

Hot-Topping Turbopump Units

The lightest turbopump unit and, therefore, the minimum rocket W_g/P for the hot-topping system was selected from figures 3(a) and 4 for each of the three chamber pressures considered. The lightest turbine-pump combinations were the ones having the highest speeds. The resulting optimum turbopump configurations are noted in the figures. The turbines selected had a limiting value of exit critical velocity ratio of 0.40. This resulted in values of turbine weight parameter of 0.69, 0.49, and 0.37 (fig. 3(a) for exit conditions of case 2) and turbopump speeds of 8430, 10,000, and 11,520 rpm for the chamber pressures of 700, 1000, and 1300, respectively. The corresponding pressure rise required for each pump was 1025, 1392, and 1807 pounds per square inch, which interpolated between the given curves in figure 4 resulted in pump weight parameters of 2.70, 2.65, and 2.82. The approximate number and type of pump stages required for the three configurations were, respectively, one inducer, one axial, one centrifugal; one inducer, four axial, one centrifugal; and one inducer, eight axial, two mixed flow. With the turbine and pump parameters combined, the turbopump weight parameter $(W_{tp}/w_p)_{HT}$ (eq. (7)) remained approximately constant for the three chamber pressures, being 3.39, 3.14, and 3.19, respectively, for chamber pressures of 700, 1000, and 1300 pounds per square inch absolute.

Values of rocket $(W_g/P)_{HT}$ (eq. (1)) were then computed for the hot-topping system for the range of missions H_f and base structural parameters $\overline{S}$ considered using the lightest turbopump unit obtained at each chamber pressure. The results are shown in figure 7(a) plotted against the structural parameter S (eq. (6)). The figure indicates the small gross-weight advantage that may be achieved by increasing the system operating pressures. The effect was due to the increase in rocket specific impulse with pressure and not to turbopump weight, which remained approximately constant. However, the exact magnitude of the saving would depend on the effects of pressure on the whole rocket system, and in this analysis only the turbopump component was considered.

Cold-Topping Turbopump Units

Because the turbine volume flow rate and radius ratio and, therefore, the required frontal area of the cold-topping turbines, was small compared with the hot-topping turbines, their speeds were higher. Just as in the hot-topping units, the lightest turbine-pump combinations for minimum rocket W_g/P had the highest speeds. These combinations

[redacted]

are noted in figures 3(b) and 4 for chamber pressures of 700 and 1000 pounds per square inch absolute. No solution was possible at the highest chamber pressure, as noted previously. The turbine weight parameters were 0.073 and 0.050 for case 2 exit conditions, and the resulting speeds were 15,510 and 18,720 rpm, respectively. The corresponding pump pressure rise was 1160 and 1943 pounds per square inch. Speeds were in the range where only axial-flow pump stages could be used for the flow rate of 800 pounds per second. A single-stage inducer was used and had to be geared down from the pump rotative speed to keep suction specific speeds from exceeding 30,000. Therefore, a parameter combining pump weight and inducer gearing weight was required rather than just a pump weight parameter as for the hot-topping units. The approximate number and type of pump stages required for the two pump configurations were, respectively: one geared inducer, eight axial; one geared inducer, fifteen axial. The resulting pump and inducer gearing weight parameters for the two units were 1.26 and 1.46, which combined with the turbine parameter gave a turbopump weight parameter of 1.33 and 1.51. The cold-topping turbopumps were less than one-half the weight of the hot-topping turbopumps.

Values of rocket $(W_g/P)_{CT}$ and structural parameter S were then computed and plotted in figure 7(b) for the lightest turbopump units obtained, in the range of chamber pressures and missions considered. Results are similar to those noted in figure 7(a) for the hot-topping system. The increase in rocket specific impulse with pressure more than counterbalanced the small increase in the cold-topping turbopump weight with pressure and resulted in a small saving in rocket gross weight with increasing pressure. However, just as in the hot-topping system, the exact magnitude of the saving would depend on the effects of pressure on the whole rocket system, whereas only the turbopump components were analyzed.

Bleed Turbopump Units

The turbine-pump combinations for the bleed turbopump units that result in the smallest addition to the gross weight of the rocket could not be selected until the effects of turbine bleed on W_g/W_e, S, and, hence, W_g/P were known (eq. (1)). To accomplish this, the rocket $(W_g/P)_B$ ratio was plotted over the range of bleed rates considered for each combination of $\bar{S}$, p_4', and H_f considered (fig. 8). The figure indicates the effect that bleed rate had on the rocket $(W_g/P)_B$. At low bleed rates, $(W_g/P)_B$ increased because of increasing turbopump weights (figs. 2 and 4). At the higher bleed rates, $(W_g/P)_B$ increased because of the increasing effect of y on I^* (eq. (36)). Minimum values of

$(W_g/P)_B$ were obtained between these two extremes, at bleed rates of 2.2, 2.7, and 3.4 percent for the three chamber pressures of 700, 1000, and 1300 pounds per square inch absolute. The value of ϵ was almost exactly 0.4 at each of these points and remained approximately constant from sea level to altitude.

The turbine configurations required to minimize $(W_g/P)_B$ are shown in figure 2. They were all eleven-stage turbines, having weight parameters of 0.59, 0.73, and 0.68 and speeds of 16,620, 14,940, and 15,490 rpm, respectively, for the three chamber pressures. The corresponding pump configurations are noted in figure 4. For pressure rises of 900, 1200, and 1500 pounds per square inch (table III) the pump plus inducer gearing weight parameters were 1.02, 1.32, and 1.54, and the approximate number and type of stages required were, respectively: one geared inducer, seven axial; one geared inducer, nine axial; one geared inducer, twelve axial. Geared inlet inducers were required as in the cold-topping pumps to keep suction specific speeds from exceeding 30,000. The overall turbopump weight parameters were 1.61, 2.05, and 2.22. The bleed turbopump units were, therefore, slightly heavier than the cold-topping units but considerably lighter than the hot-topping units.

In figure 9, rocket $(W_g/P)_B$ is shown plotted against the structural parameter S at the bleed rates corresponding to the minimum $(W_g/P)_B$ points in the previous figure. It may be seen that chamber pressure had almost no effect on $(W_g/P)_B$ for a given value of S. The effects of increasing turbopump weight and bleed rate with chamber pressure approximately equaled the effects of increasing specific impulse with chamber pressure. However, the effect of pressure on the remainder of the rocket system $\bar{S}$ was not considered in this analysis, and, therefore, the total effect of pressure on $(W_g/P)_B$ can not be obtained from the figure.

SUMMARY OF RESULTS

An analysis was made of three types of turbopump units designed for application to a nuclear hydrogen rocket. The results are summarized in the following table, giving the turbopump configurations required to minimize the rocket ratio of gross weight to payload (W_g/P) for each system. The designs were for turbine tip speeds of 1400 feet per second and pumps scaled to a flow rate of 800 pounds per second.

Type of turbine	Chamber pressure, p_4^i, lb/sq in. abs (a)	Ratio of turbine to pump flow, y, percent	Number of turbine stages, n	Rotative speed, N, rpm	Pump pressure rise, Δp_p^i, lb/sq in.	Pump stages (b)	Ratio of turbo-pump weight to pump weight flow, W_{tp}/w_p
Bleed	700	2.2	11	16,620	900	1 geared I + 7A	1.61
	1000	2.7	11	14,940	1200	1 geared I + 9A	2.05
	1300	3.4	11	15,490	1500	1 geared I + 12A	2.22
Cold topping	700	[a]80	1	15,510	1160	1 geared I + 8A	1.33
	1000	80	1	18,720	1943	1 geared I + 15A	1.51
	1300	80	1	------	∞	----------	----
Hot topping	700	80	1	8,430	1025	1I + 1A + 1C	3.39
	1000	80	1	10,000	1393	1I + 4A + 1C	3.14
	1300	80	1	11,520	1807	1I + 8A + 2M	3.19

[a]Values arbitrarily selected for the analysis.

[b]I, inducer; M, mixed; A, axial; C, centrifugal.

The items listed in the table are applicable over the range of missions and rocket base structural parameters considered in the analysis. No turbopump designs were feasible for the highest pressure cold-topping system considered. The power required to drive the pump exceeded the available energy of the turbine drive fluid for the given system operating conditions.

The high blade bending forces imposed on the single-stage topping turbines would have exceeded the material stress limits if conventional rigidly mounted radial blades were used. Therefore, it was assumed that blade attachments could be made to allow for enough blade lean to counterbalance the bending forces.

Consideration of the effect of turbopump configuration alone indicates differences in payload of the order of 2 to 12 percent. These differences appear small in comparison with possible effects of the turbopump configurations on weight of associated components such as the reactor. It is indicated, therefore, that the final selection of the turbopump system will include other considerations, such as the effect of the turbopump system on starting and control, as well as the effect on reactor and other component weights. These considerations were not within the scope of the analysis.

National Aeronautics and Space Administration
Lewis Research Center
Cleveland, Ohio, March 22, 1960

REFERENCES

1. Hilsenrath, Joseph, et al.: Tables of Thermal Properties of Gases. Cir. 564, NBS, Nov. 1, 1955.

2. Stewart, Warner L., Evans, David G., and Whitney, Warren J.: A Method for Determining Turbine Design Characteristics for Rocket Turbodrive Applications. NACA RM E57K25a, 1958.

3. Stewart, Warner L.: Analytical Investigation of Multistage-Turbine Efficiency Characteristics in Terms of Work and Speed Requirements. NACA RM E57K22b, 1958.

4. Rohlik, Harold E., and Crouse, James E.: Analytical Investigation of the Effect of Turbopump Design on Gross-Weight Characteristics of a Hydrogen-Propelled Nuclear Rocket. NASA MEMO 5-12-59E, 1959.

5. Sutton, George P.: Rocket Propulsion Elements. Second ed., John Wiley & Sons, Inc., 1956.

TABLE I. - ASSUMED TEMPERATURES, PRESSURES, AND FLOW RATES

Condition	Bleed system	Topping system	
		Hot	Cold
Turbine-inlet temperature, T_2', $^{\circ}R$	1860	1860	560
Chamber temperature, T_4', $^{\circ}R$	3960	3960	3960
Pump inlet pressure, p_0', lb/sq in. abs	35	35	35
Pump flow rate, w_p, lb/sec	800	800	800
Chamber pressure, p_4', lb/sq in. abs	700,1000,1300	700,1000,1300	700,1000,1300
Turbine- to pump-flow ratio, y	0.02 to 0.06	0.80	0.80

TABLE II. - LINE TOTAL-PRESSURE LOSS

Loss between stations	Total-pressure loss, lb/sq in.		
	Bleed system	Topping system	
		Hot	Cold
1 and 2	200	200	190
1 and 4	[a]235	[b]245	[b]245
3 and 5_{tn}	15	---	---
4 and 5	10	10	10

[a]Exclusive of turbine (station 2 to 3).

[b]Exclusive of turbine (station 2 to 3a).

TABLE III. - PUMP PRESSURE RISE

Nozzle chamber pressure, p_4', lb/sq in. abs	Pressure rise, $\Delta p_p'$, lb/sq in.		
	Bleed system	Topping system	
		Hot	Cold
700	900	$165 + 745(p_2'/p_{3a}')$	$155 + 755(p_2'/p_{3a}')$
1000	1200	$165 + 1045(p_2'/p_{3a}')$	$155 + 1055(p_2'/p_{3a}')$
1300	1500	$165 + 1345(p_2'/p_{3a}')$	$155 + 1355(p_2'/p_{3a}')$

TABLE IV. - CONDITIONS ASSUMED IN SOLUTION OF $(W_t/w_p)_B$ FOR THE BLEED TURBINE

Overall pump efficiency, η_p	0.70
Turbine-inlet temperature, T_2', $^\circ R$	1860
Turbine tip speed, U, ft/sec	1400
Turbine-exit axial- to critical-velocity ratio, $\left(\frac{V_x}{V_{cr}}\right)_3$	0.40
Turbine blade hub- to tip-radius ratio, $\left(\frac{r_h}{r_t}\right)_3$	0.80
Turbine weight factor, K	70
Pump pressure rise, $\Delta p_p'$, lb/sq in. (table III)	900,1200,1500
Ratio of turbine to pump weight-flow rate, y	0.02 to 0.06
Number of turbine stages, n	2-12
Ratio of specific heats, γ	1.38
Specific heat at constant pressure, c_p, Btu/(lb)($^\circ R$)	3.5
Propellant density, ρ_p, lb/cu ft	4.42

TABLE V. - CONDITIONS ASSUMED IN SOLUTION OF $(W_t/w_p)_T$ FOR TOPPING TURBINE

	Cold topping	Hot topping
Turbine-inlet temperature, T_2', $^\circ R$	560	1860
Turbine tip speed, U, ft/sec	1400	1400
Ratio of turbine to pump weight-flow rate, y	0.80	0.80
Number of turbine stages, n	1	1
Turbine blade hub- to tip-radius ratio, $\left(\frac{r_h}{r_t}\right)_3$	0.60	0.80
Turbine-exit axial- to critical-velocity ratio, $\left(\frac{V_x}{V_{cr}}\right)_3$	0.10-0.40	0.10-0.40
Turbine weight factor, K	25	70
Pump pressure rise, $\Delta p_p'$, lb/sq in.	See table III	See table III
Overall pump efficiency, η_p	0.70	0.70
Ratio of specific heats, γ	1.40	1.38
Specific heat at constant pressure, c_p, Btu/(lb)($^\circ R$)	3.3	3.5
Propellant density, ρ_p, lb/cu ft	4.42	4.42
Material	Aluminum	Steel alloy

[redacted]

TABLE VI. - DESIGN CONDITIONS FOR PUMPS OF REFERENCE 4

Parameter	Pump type		
	Axial flow	Mixed flow	Centrifugal
Pump pressure rise, $\Delta p'_p$, lb/sq in.	1150	1150	1150
Rotative speed, N, rpm	20,000	20,000	16,000
Suction specific speed, ss	19,400	19,400	15,500
Pump weight flow, w_p, lb/sec	360	360	360
Pump weight parameter, W_p/w_p	1.01	0.86	1.05
Number of pump stages, n	8	2	2

TABLE VII. - BURNOUT TIMES AND WEIGHT RATIOS

Final altitude, H_f, ft	Chamber pressure, p'_4, lb/sq in.	Burnout time, t_{BO}, sec	Gross- to empty-weight ratio, W_g/W_e
65×10^5	700	246.4	2.995
	1000	258.6	2.980
	1300	267.4	2.972
110×10^5	700	276.8	3.975
	1000	290.6	3.953
	1300	300.9	3.935
155×10^5	700	295.2	4.968
	1000	310.4	4.930
	1300	321.1	4.905

TABLE VIII. - EXAMPLE BLEED SYSTEM

[Turbine- to pump-flow ratio y, 0.04; number of turbine stages n, 4; nozzle chamber pressure p'_4, 700 lb/sq in. abs; rocket base structural parameter $\overline{S}$, 0.15; total mission altitude H_f, 110×10^5 ft.]

Step	Property	Value	Source
	Turbopump calculations		
1	$\Delta p'_p$, lb/sq in.	900	Table III
2	y	0.04	Selected
3	ρ_p, lb/cu ft	4.42	Table IV
4	η_p	0.70	Table IV
5	J, ft-lb/Btu	778.2	----------
6	$\Delta h'$, Btu/lb	1346	Steps 1 to 5 and eq. (11)
7	U, ft/sec	1400	Constant for analysis
8	g, ft/sec^2	32.2	Constant for analysis
9	n	4	Selected
10	η_t	0.66	Steps 5 to 9 and ref. 2
11	T'_2, $^\circ R$	1860	Table IV
12	c_p, Btu/(lb)($^\circ$R)	3.5	Table IV
13	γ	1.38	Table IV
	Rocket and mission calculations		
26	H_f,	110×10^5	Selected
27	V_f, ft/sec	0	Constant for analysis
28	G	1.4	Constant for analysis
29	$p'_{4,rn} = p_{4,rn}$, lb/sq in. abs	700	Selected
30	$p_{5,rn}$, lb/sq ft abs	243	Ref. 5
31	$p'_{5,rn}$, lb/sq in. abs	690	Step 29 and table II
32	$(A/A_{cr})_{5,rn}$	26.7	Ref. 5
33	γ_{rn}	1.30	Assumed
34	δ_{rn}	0.94	Assumed
35	$p_{4,th} = p'_{4,th} = p'_{5,th}$, lb/sq in. abs	173	Steps 14 and 18 and table II

Step	Property	Value	Source
14	p_3/p'_2	0.256	Steps 6 and 10 to 13 and eq. (12)
15	K	70	Table IV
16	$(r_h/r_t)_3$	0.80	Table IV
17	$(V_x/V_{cr})_3$	0.40	Table IV
18	p'_2, lb/sq in. abs	735	Tables I to III
19	R, $ft/^\circ R$	767	Ref. 1
20	W_t/w_p, (lb)(sec)/lb	0.24	Steps 2, 6 to 9, and 11 to 19, ref. 2, and eq. (10)
21	w_p, lb/sec	800	Table I
22	$N_t = N_p$, rpm	20,210	Steps 7, 9, 15, 20, and 21 and eq. (18)
23	$\frac{W_p + W_G}{w_p}$, (lb)(sec)/lb	1.09	Steps 1 and 22 and fig. 4
24	W_{tp}/w_p, (lb)(sec)/lb	1.33	Steps 20 and 23 and eq. (7)
25	$T'_{4,th}$, $^\circ R$	1475	Steps 6, 11, and 12 and eq. (35)
36	δ_{tn}	0.97	Assumed
37	γ_{tn}	1.38	Assumed
38	t_{BO}, sec	273.9	Steps 2, 8, 19, 25,26, and 28 to 37, ref. 5, and simultaneous solution of eqs. (22), (24) to (34), (36), and (37)
39	I^*_{sl}, sec	509	Steps 2, 8, 19, 25,26, and 28 to 37, ref. 5, and simultaneous solution of eqs. (22), (24) to (34), (36), and (37)
40	I^*_{BO}, sec	747	Steps 2, 8, 19, 25,26, and 28 to 37, ref. 5, and simultaneous solution of eqs. (22), (24) to (34), (36), and (37)
41	ϵ_{sl}	0.57	Steps 2, 8, 19, 25,26, and 28 to 37, ref. 5, and simultaneous solution of eqs. (22), (24) to (34), (36), and (37)
42	ϵ_{BO}	0.41	Steps 2, 8, 19, 25,26, and 28 to 37, ref. 5, and simultaneous solution of eqs. (22), (24) to (34), (36), and (37)
43	W_g/W_e	4.06	Steps 28, 38, and eq. (39)
44	$\overline{S}$	0.15	Selected
45	$W_{tp}/w_p t_{BO}$	0.00486	Steps 24, 38, and 44 and eq. (6)
46	S	0.15486	Steps 24, 38, and 44 and eq. (6)
47	W_g/P	7.72	Steps 43 and 46 and eq. (1)

[redacted]

TABLE IX. - EXAMPLE COLD-TOPPING SYSTEM

[Turbine-exit blade radius ratio $(r_h/r_t)_3$, 0.60; turbine-exit axial- to critical-velocity ratio $(V_x/V_{cr})_3$, 0.40; turbine-exit pressure loss (case 2) p_3/p'_{3a}, 1.0; rocket base structural parameter $\overline{S}$, 0.15; total mission altitude H_f, 110×10^5 ft; nozzle chamber pressure p'_4, 700 lb/sq in. abs.]

Step	Property	Value	Source	Step	Property	Value	Source
Turbopump calculations							
1	$\Delta p'_p$, lb/sq in.	1160	Step 16 and table III	14	p'_3/p'_2	0.826	Steps 6, 10 to 13 and eq. (15)
2	y	0.80	Constant for topping analysis	15	$(V_x/V_{cr})_3$	0.40	Selected
3	ρ_p, lb/cu ft	4.42	Table V	16	$\frac{p_3}{p'_2} = \frac{p'_{3a}}{p'_2}$	0.752	Steps 13 to 15 and eqs. (13), (14), and (17)
4	η_p	0.70	Table V	17	K	25	Table V
5	J, ft-lb/Btu	778.2	----------	18	r_h/r_t	0.60	Selected
6	$\Delta h'$, Btu/lb	86	Steps 1 to 5 and eq. (11)	19	p'_2, lb/sq in. abs	1005	Step 1 and tables I and II
7	U, ft/sec	1400	Constant for analysis	20	R, ft/^oR	767	Ref. 1
8	g, ft/sec^2	32.2	Constant for analysis	21	W_t/w_p (lb)(sec)/lb	0.073	Steps 2, 6, 8, 9, 11 to 13 and 15 to 20, ref. 2, and eq. (10)
9	n	1	Constant for topping analysis	22	w_p, lb/sec	800	Table I
10	$\overline{\eta}_t$	0.87	Steps 5 to 9 and eq. (16) of ref. 3	23	$N_t = N_p$, rpm	15,510	Steps 7, 9, 17, 21, and 22 and eq. (18)
11	T'_2, ^oR	560	Table V	24	W_p/w_p, (lb)(sec)/lb	1.26	Steps 1 and 23 and fig. 3
12	c_p, Btu/(lb)(^oR)	3.3	Table V	25	W_{tp}/w_p, (lb)(sec)/lb	1.33	Steps 21 and 24 and eq. (7)
13	γ	1.40	Table V				
Rocket and mission calculations							
26	H_f, ft	110×10^5	Selected	35	t_{BO}, sec	276.8	Steps 2, 8, 20, 26, and 28 to 34, ref. 5, and simultaneous solution of eqs. (22), (24) to (31), and (38)
27	V_f, ft/sec	0	Constant for analysis	36	I^*_{s1}, sec	518	
28	G	1.4	Constant for analysis	37	I^*_{BO}, sec	763	
29	$p'_{4,rn} = p_{4,rn}$, lb/sq in. abs	700	Selected	38	W_g/W_e	3.97	Steps 28, 35, and 36 and eq. (39)
30	$p_{5,rn}$, lb/sq ft abs	243	Ref. 5	39	$\overline{S}$	0.15	Selected
31	$p'_{5,rn}$, lb/sq in. abs	690	Step 29 and table II	40	$W_{tp}/w_p t_{BO}$	0.0048	Steps 25, 35, and 39 and eq. (6)
				41	S	0.1548	
32	$(A/A_{cr})_{5,rn}$	26.7	Ref. 5	42	W_g/P	7.35	Steps 38 and 41 and eq. (1)
33	γ_{rn}	1.30	Assumed				
34	δ_{rn}	0.94	Assumed				

[redacted]

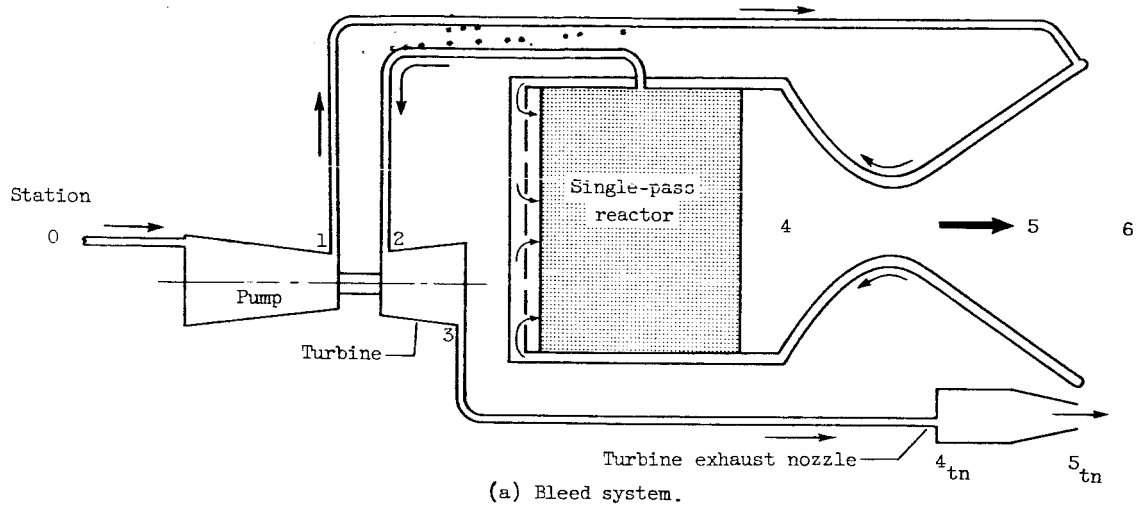

(a) Bleed system.

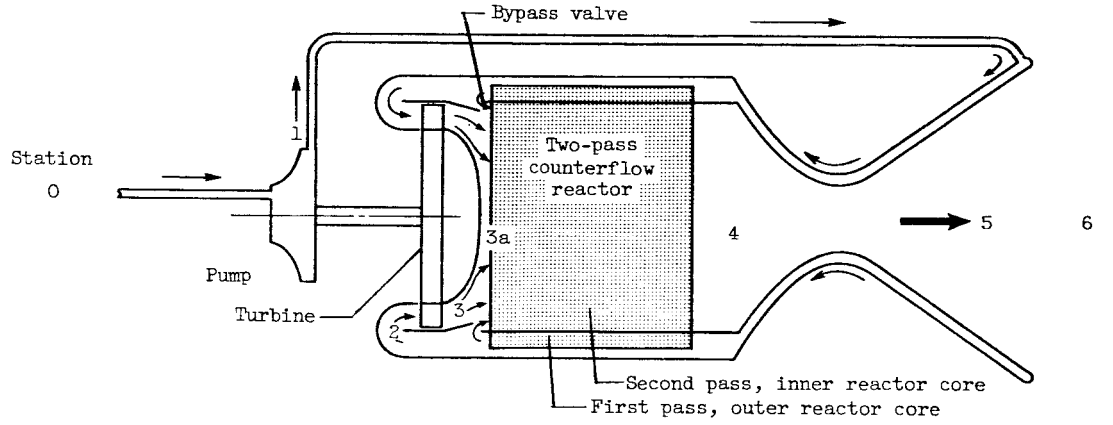

(b) Hot-topping system.

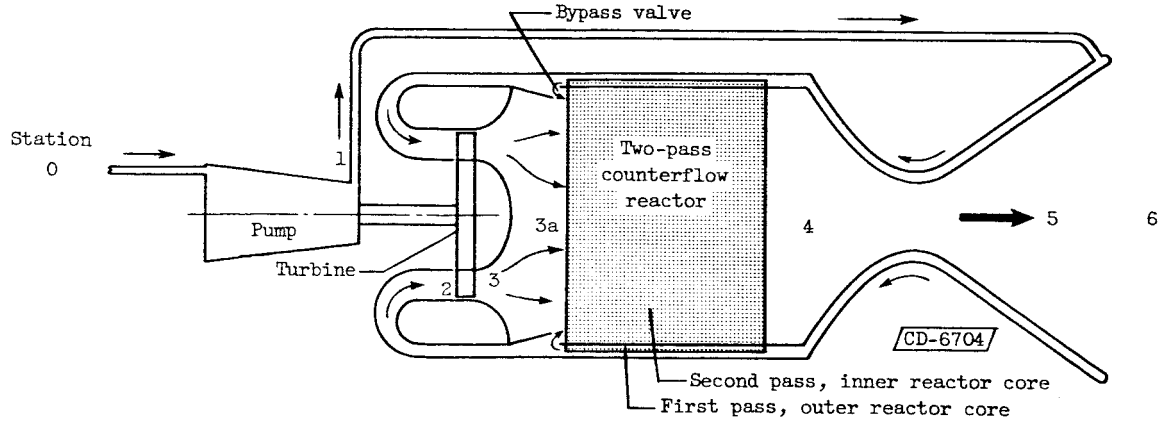

(c) Cold-topping sytem.

Figure 1. - Schematic diagrams of three turbopump systems investigated.

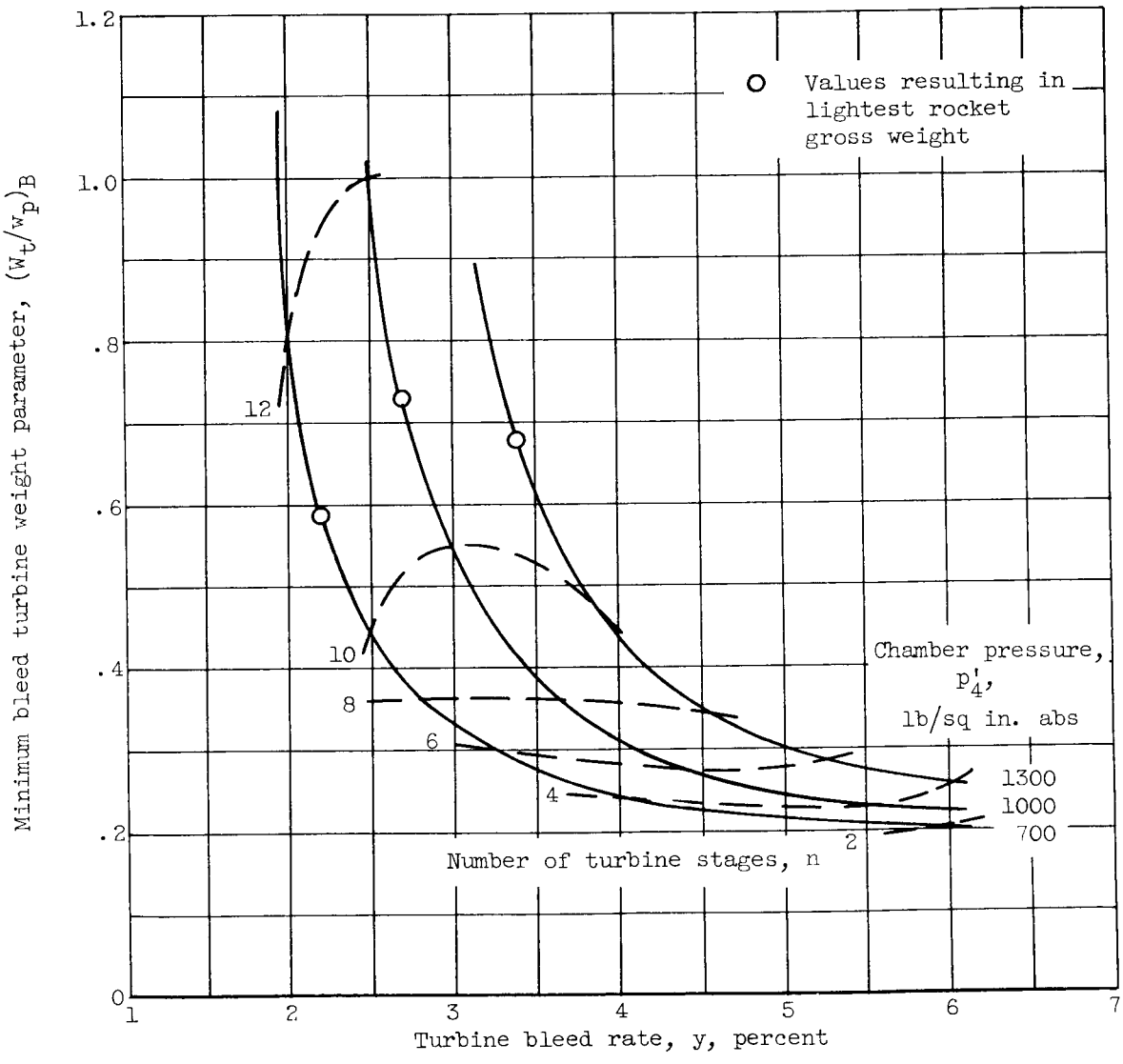

Figure 2. - Variation of turbine weight parameter with bleed rate for range of turbine stages and chamber pressures for bleed turbopump system.

E-581

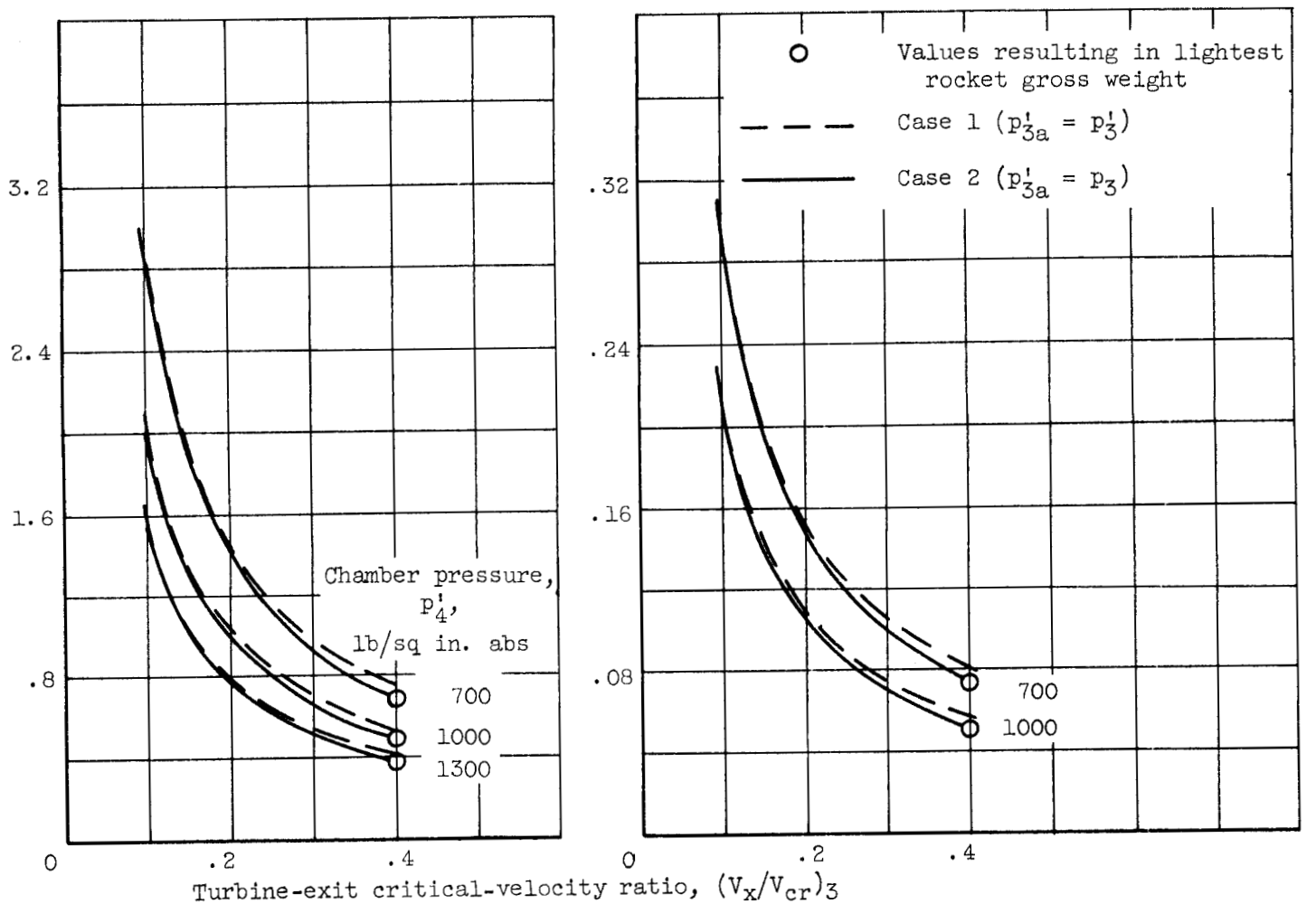

(a) Hot-topping unit. (b) Cold-topping unit.

Figure 3. - Variation of turbine weight parameter with critical-velocity ratio for range of chamber pressures and turbine-exit velocity head loss assumptions for two topping turbopump systems.

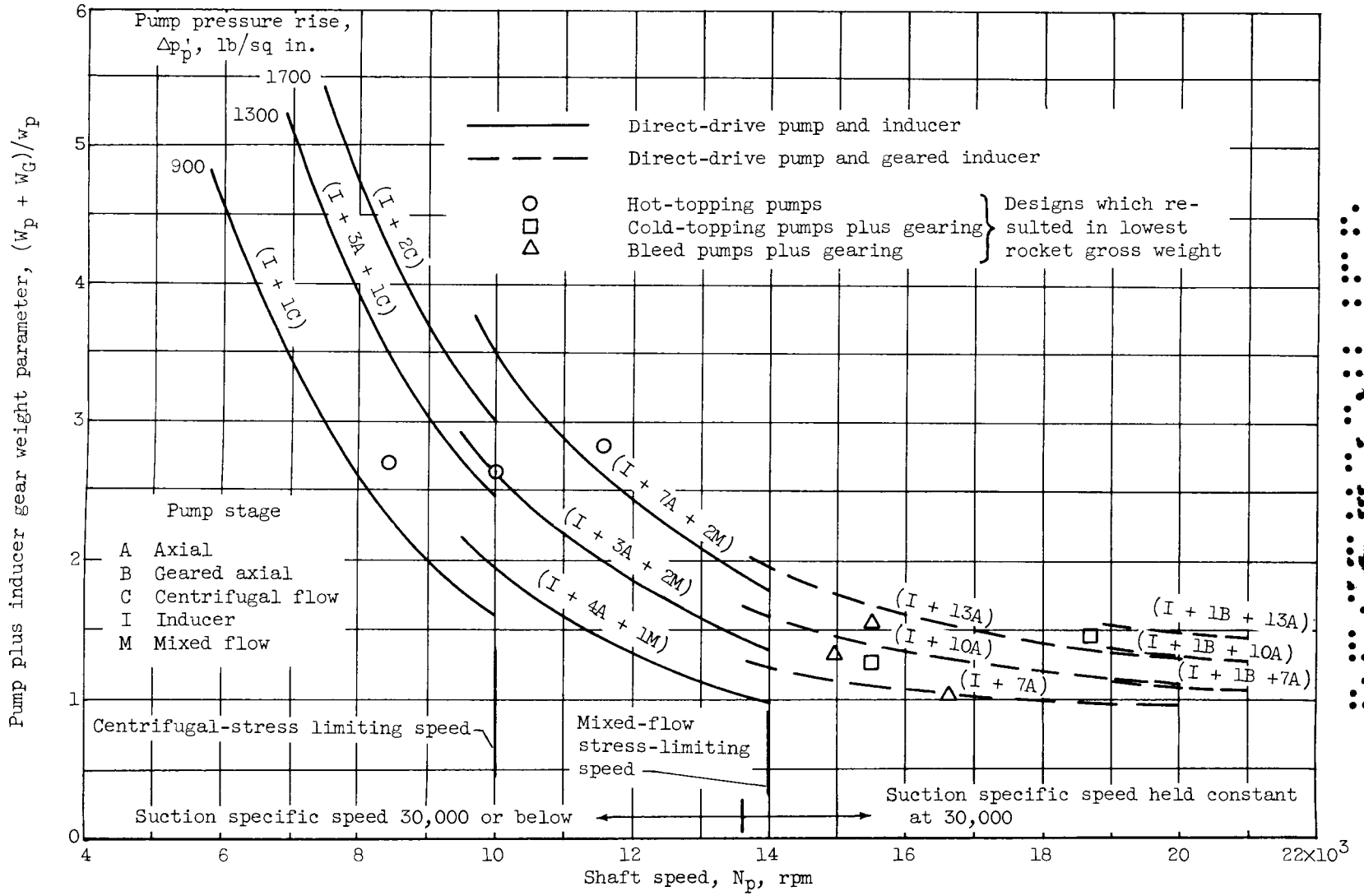

Figure 4. - Variation of pump plus inducer gear weight parameter with shaft speed for pump pressure rises of 900, 1300, and 1700 pounds per square inch. Flow rate, 800 pounds per second; liquid hydrogen.

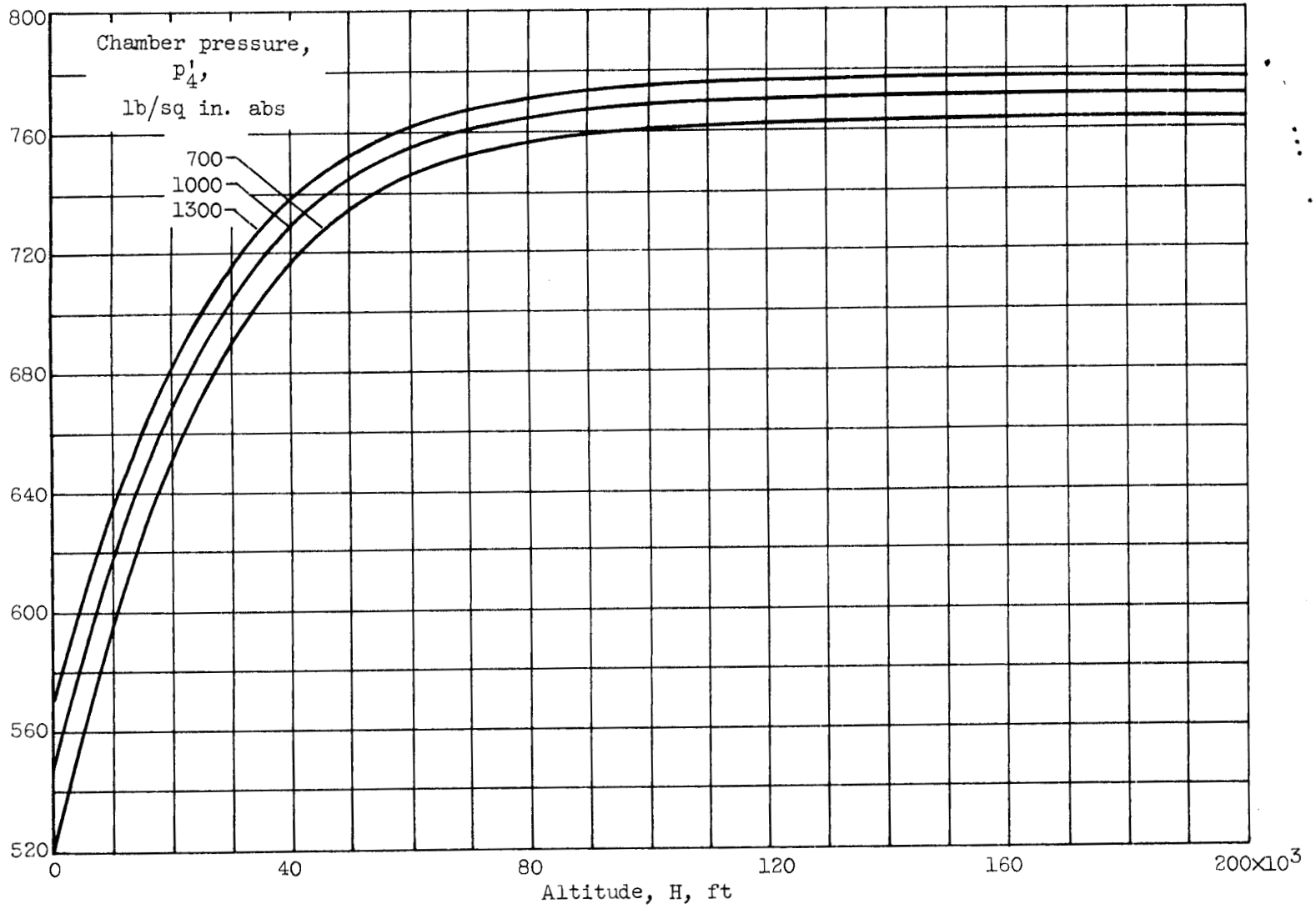

Figure 5. - Variation of nozzle specific impulse with altitude at chamber pressures of 700, 1000, and 1300 pounds per square inch absolute.

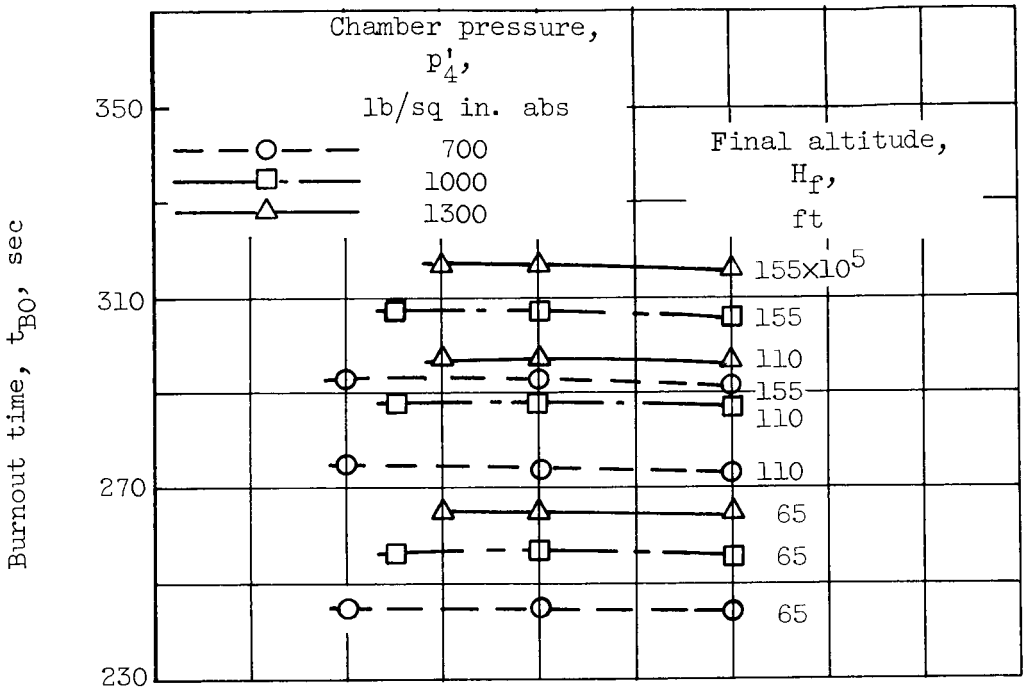

(a) Rocket burnout time.

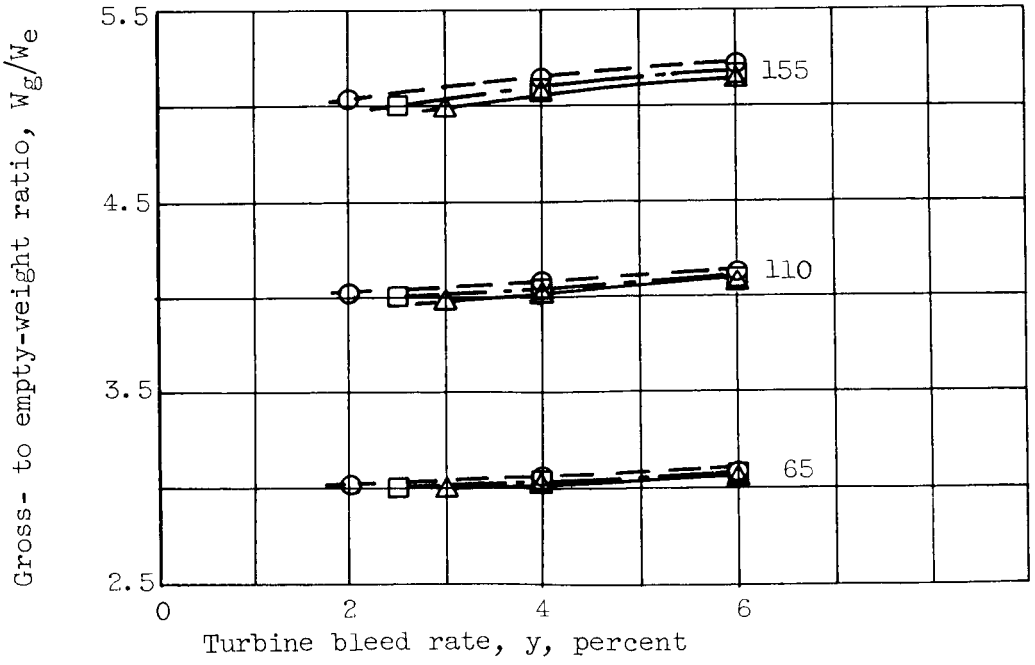

(b) Rocket gross- to empty-weight ratio.

Figure 6. - Variation of rocket burning time and gross- to empty-weight ratio with turbine bleed over range of rocket missions and chamber pressures.

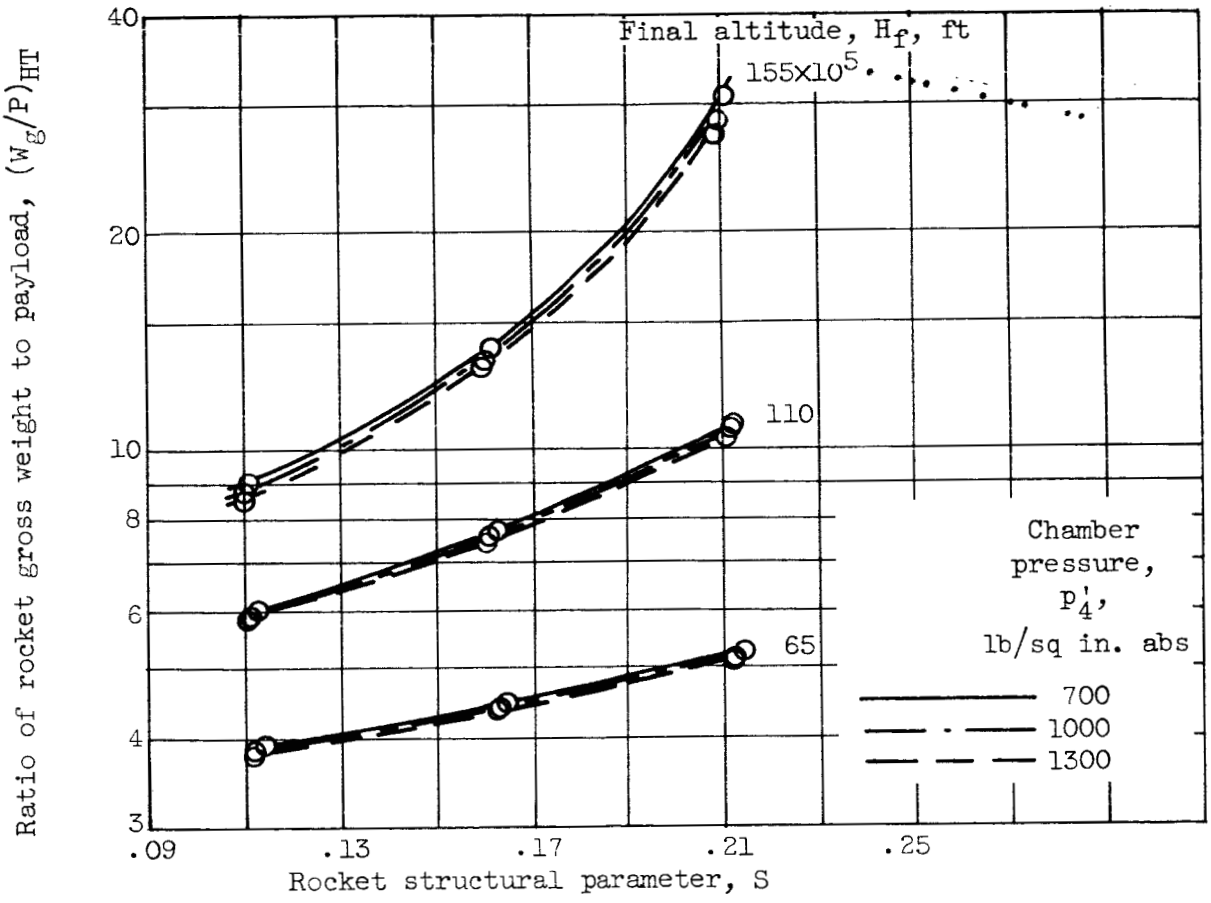

(a) Hot-topping turbopump.

Figure 7. - Variation of ratio of rocket gross weight to payload with structural parameter using minimum-weight turbopump units over range of missions and chamber pressures.

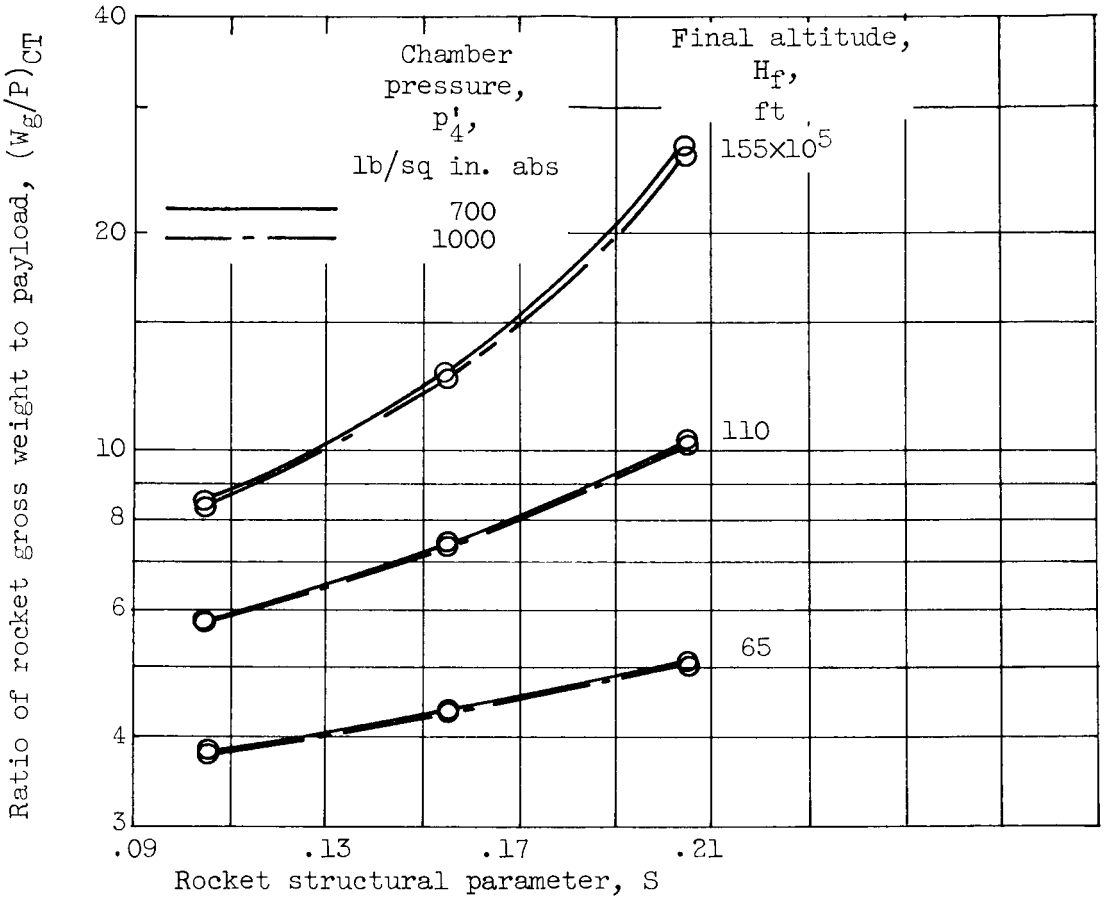

(b) Cold-topping turbopump.

Figure 7. - Concluded. Variation of ratio of rocket gross weight to payload with structural parameter using minimum-weight turbopump units over the range of missions and chamber pressures.

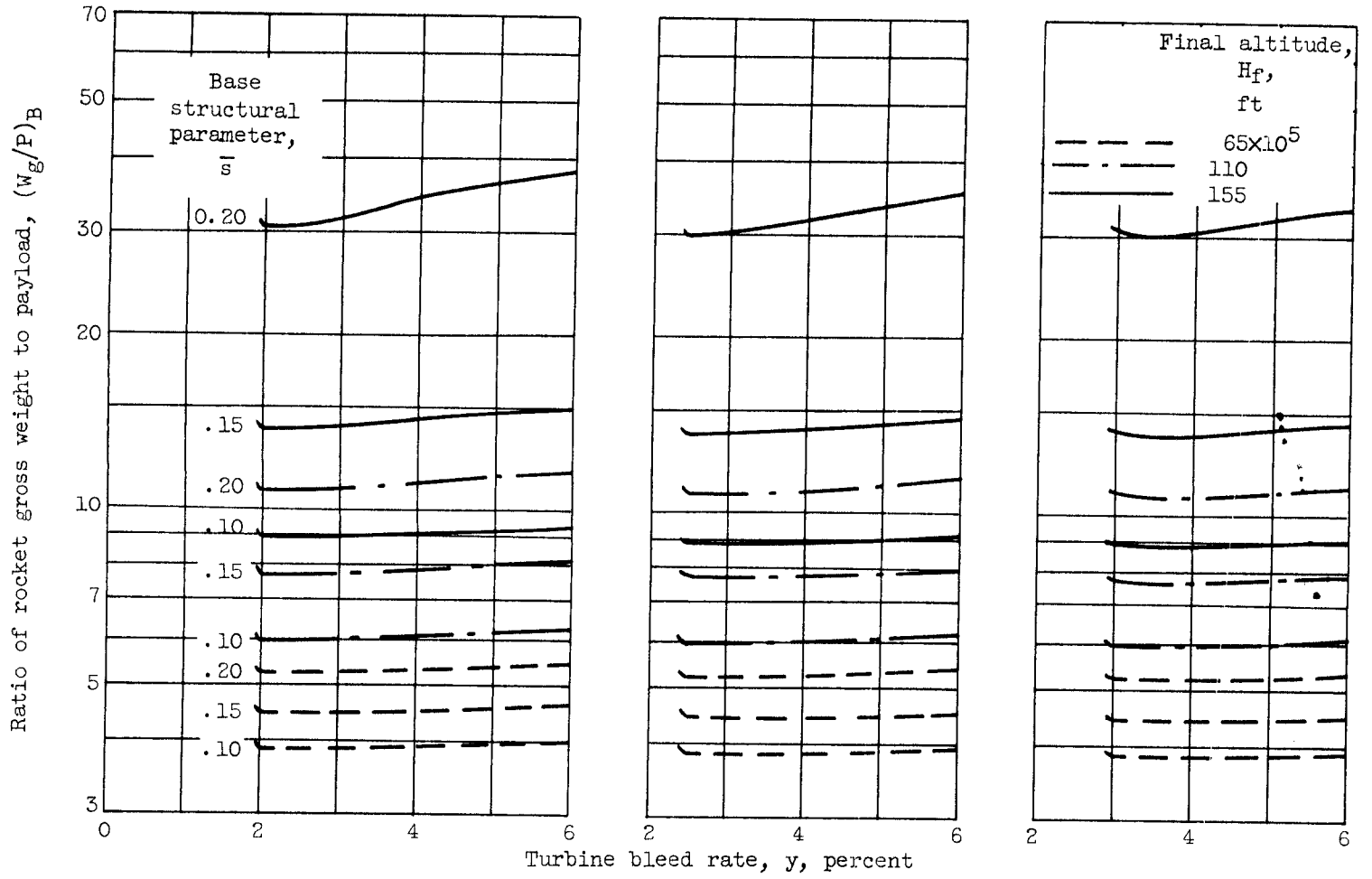

(a) Chamber pressure, 700 pounds per square inch absolute.

(b) Chamber pressure, 1000 pounds per square inch absolute.

(c) Chamber pressure, 1300 pounds per square inch absolute.

Figure 8. - Variation of ratio of rocket gross weight to payload with bleed rate for range of chamber pressures, base structural parameters, and missions for bleed turbopump system.

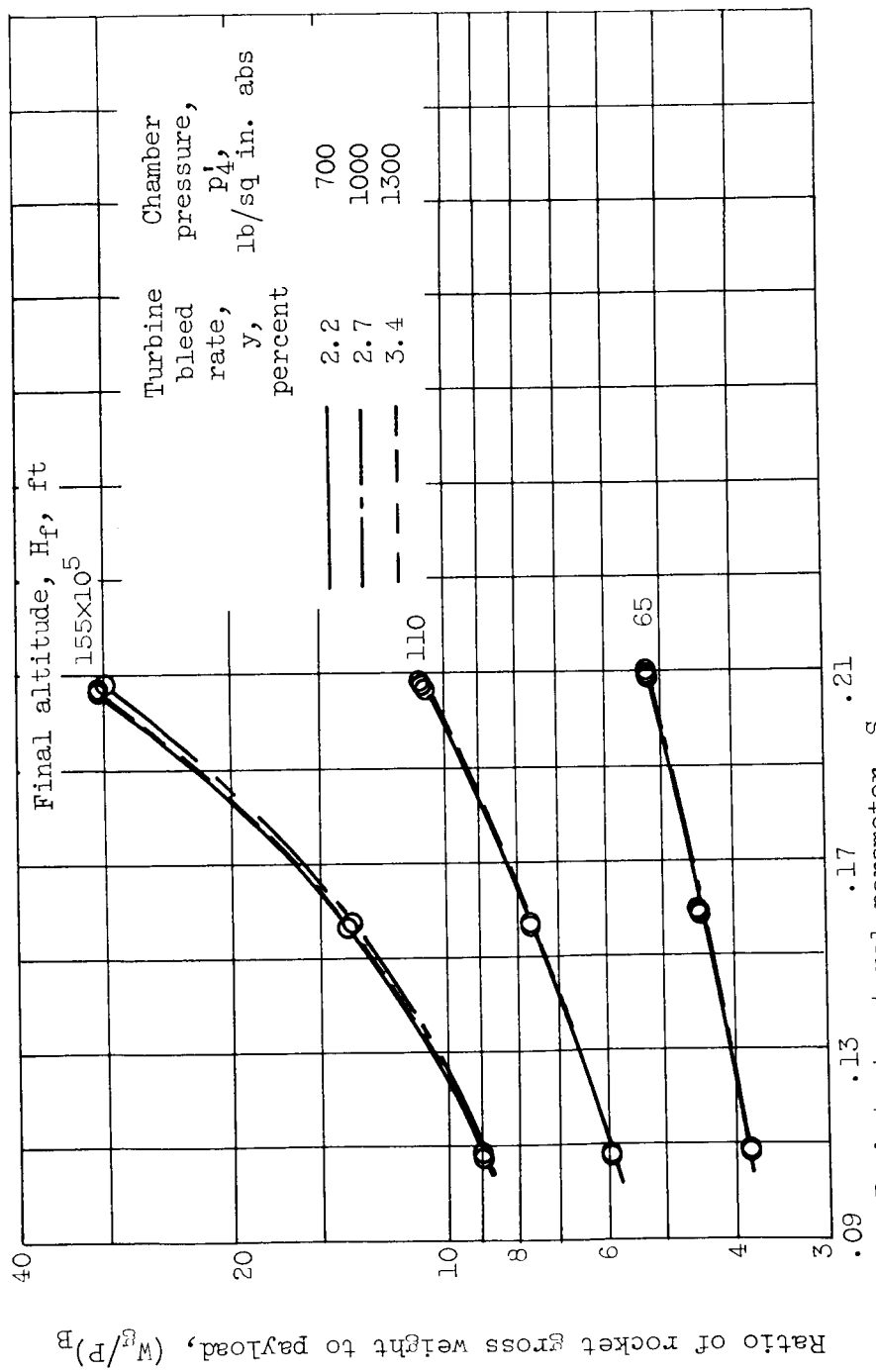

Figure 9. - Variation of ratio of rocket gross weight to payload with structural parameter for minimum-weight bleed turbopump system for range of missions and chamber pressures.